

**Nanofabricated structures and microfluidic devices for bacteria  
From techniques to biology**

Wu, Fabai; Dekker, Cees

**DOI**

[10.1039/c5cs00514k](https://doi.org/10.1039/c5cs00514k)

**Publication date**

2016

**Document Version**

Accepted author manuscript

**Published in**

Chemical Society Reviews

**Citation (APA)**

Wu, F., & Dekker, C. (2016). Nanofabricated structures and microfluidic devices for bacteria: From techniques to biology. *Chemical Society Reviews*, 45(2), 268-280. <https://doi.org/10.1039/c5cs00514k>

**Important note**

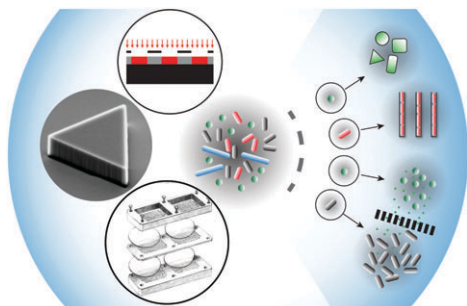
To cite this publication, please use the final published version (if applicable).  
Please check the document version above.

**Copyright**

Other than for strictly personal use, it is not permitted to download, forward or distribute the text or part of it, without the consent of the author(s) and/or copyright holder(s), unless the work is under an open content license such as Creative Commons.

**Takedown policy**

Please contact us and provide details if you believe this document breaches copyrights.  
We will remove access to the work immediately and investigate your claim.



### Nanofabricated structures and microfluidic devices for bacteria: from techniques to biology

Fabai Wu and Cees Dekker\*

We review the use of nanofabricated structures and microfluidic technologies that spatially separate bacteria for quantitative analyses and that provide topological constraints on their growth and chemical communications.

Q1  
Q2

Please check this proof carefully. **Our staff will not read it in detail after you have returned it.**

Translation errors between word-processor files and typesetting systems can occur so the whole proof needs to be read. Please pay particular attention to: tabulated material; equations; numerical data; figures and graphics; and references. If you have not already indicated the corresponding author(s) please mark their name(s) with an asterisk. Please e-mail a list of corrections or the PDF with electronic notes attached – do not change the text within the PDF file or send a revised manuscript. Corrections at this stage should be minor and not involve extensive changes. All corrections must be sent at the same time.

**Please bear in mind that minor layout improvements, e.g. in line breaking, table widths and graphic placement, are routinely applied to the final version.**

Please note that, in the typefaces we use, an italic vee looks like this:  $\nu$ , and a Greek nu looks like this:  $\nu$ .

We will publish articles on the web as soon as possible after receiving your corrections; **no late corrections will be made.**

Please return your **final** corrections, where possible within **48 hours** of receipt, by e-mail to: chemsocrev@rsc.org

## Queries for the attention of the authors

Journal: **Chem Soc Rev**

Paper: **c5cs00514k**

Title: **Nanofabricated structures and microfluidic devices for bacteria: from techniques to biology**

Editor's queries are marked on your proof like this **Q1**, **Q2**, etc. and for your convenience line numbers are indicated like this 5, 10, 15, ...

Please ensure that all queries are answered when returning your proof corrections so that publication of your article is not delayed.

<b>Query reference</b>	<b>Query</b>	<b>Remarks</b>
Q1	For your information: You can cite this article before you receive notification of the page numbers by using the following format: (authors), Chem. Soc. Rev., (year), DOI: 10.1039/c5cs00514k.	
Q2	Please carefully check the spelling of all author names. This is important for the correct indexing and future citation of your article. No late corrections can be made.	
Q3	Ref. 4 and 17: Please provide the page (or article) numbers.	
Q4	Ref. 42: Can this reference be updated?	

# Nanofabricated structures and microfluidic devices for bacteria: from techniques to biology

Cite this: DOI: 10.1039/c5cs00514k

Fabai Wu and Cees Dekker\*

Nanofabricated structures and microfluidic technologies are increasingly being used to study bacteria because of their precise spatial and temporal control. They have facilitated studying many long-standing questions regarding growth, chemotaxis and cell-fate switching, and opened up new areas such as probing the effect of boundary geometries on the subcellular structure and social behavior of bacteria. We review the use of nano/microfabricated structures that spatially separate bacteria for quantitative analyses and that provide topological constraints on their growth and chemical communications. These approaches are becoming modular and broadly applicable, and show a strong potential for dissecting the complex life of bacteria at various scales and engineering synthetic microbial societies.

Received 30th June 2015

DOI: 10.1039/c5cs00514k

[www.rsc.org/chemsocrev](http://www.rsc.org/chemsocrev)

## Key learning points

- (1) Microfabricated structures can spatially isolate and separate bacteria for single-cell analyses, for drug discovery by cultivating natural species on chips, and for lineage tracking that reveals the rules governing cell growth, cell-fate decisions, and antibiotic resistance.
- (2) Microfluidic devices that separate bacteria with semipermeable materials allow dissecting the effect of chemical communication between bacteria that exchange metabolic compounds, signaling molecules, and antibiotic resistance.
- (3) Microhabitats can be fabricated with defined geometric features that constrain the growth patterns and social behavior of bacteria, leading to spatially structured populations that show rapid adaptation to environmental stress.
- (4) Nanofabricated microchambers can be used to 'sculpt' bacteria into defined shapes and sizes for investigating the spatial adaptation of their subcellular organization, such as how lipids sense curvatures and how cell-division-related proteins form patterns to find symmetry axes and adapt to cell sizes.
- (5) The combination of microfluidics and synthetic genetic circuits allows for engineering synthetic microbial societies capable of organizing into defined structures and executing controllable functions.

Biology is a study of living matter in space and time. Nanotechnology provides tools that manipulate materials in space and time with an exquisite amount of detail. With biology entering the quantitative era, there is an increasing demand for systematic and precise control over the spatial and temporal parameters in experiments. It therefore is becoming very appealing for biologists to pick up the toolkits from nanotechnology, such as nanofabricated structures and microfluidic technologies.

Much fundamental knowledge of biology is garnered through studying bacteria. While any organism exhibits an impressive amount of complexity, a bacterium is generally simpler than a eukaryote regarding its metabolic, signaling, and architectural networks. Hence, it is considerably easier to break down these networks into modules feasible for analysis and engineering. The versatile metabolic capacities shown in the bacterial kingdom represent a rich pool of resources, which have the potential of

significantly contributing to solving the major issues of the world such as food, energy, and medicine. In Nature, bacteria play indispensable roles in ecosystems such as soil and human bodies. Moreover, they can be infectious agents that cause persistent medical problems. So far, our ability to cultivate bacteria, to harness their power as well as to extinguish them at will is far from satisfactory. This is largely due to our limited understanding of bacteria at many levels, from the orchestration of their inner structure to the rules governing their social behavior.

Nano- and microfabricated structures offer unique features to obtain previously inaccessible knowledge about bacteria. The spatial scales that can be manipulated by various lithography and etching techniques range from nanometer to centimeter sizes (Fig. 1A and B), that is, from the size of a protein cluster on the cell membrane to the size of a bacterial colony. The volume and pressure control provided by microfluidics enables rapid changes as well as long-term maintenance of defined chemical and physical environments for bacteria<sup>1</sup> (Fig. 1B). Using these techniques, it is now possible to sort single bacterial cells from a soil or blood sample and designate them

*Delft University of Technology, Department of Bionanoscience, Kavli Institute of Nanoscience Delft, Lorentzweg 1, 2628CJ Delft, The Netherlands.  
E-mail: c.dekker@tudelft.nl*

1 into individual compartments, where they can be separately  
cultivated, monitored and manipulated (Fig. 1C).

5 In this tutorial review, we introduce the application of nano- and  
microfabricated structures in bacteria by categorizing their func-  
tional purposes. We hope that such an overview will facilitate more  
microbiologists to pick up the experimental toolkits that are best  
suited for their applications (Fig. 1C) and that will encourage further  
collaborations between microbiologists and nanoengineers. We  
start by introducing the major classes of fabrication techniques  
10 (Fig. 1A) and several essential elements that are in common use for  
applications in bacteria (Fig. 1B). Subsequently, we describe high-  
throughput applications realized by separating bacteria (Fig. 1C,  
panel 1), which lead us to the subsequent long-term tracking of  
lineages (Fig. 1C, panel 2). Following spatial separation, the means  
15 to bring populations into chemical communication is introduced  
(Fig. 1C, panel 2). We then address the functional role of geometry  
at various spatial scales by presenting several global and local  
geometric features that illuminated the growth and adaptation of  
bacteria in space (Fig. 1C, panel 2). Zooming in further, we peek into  
20 the potential of cell-shaping techniques for studying subcellular  
organization (Fig. 1C, panel 3). Finally, we provide a brief outlook  
into the future opportunities and challenges of applying nanofab-  
ricated structures to studying bacteria.

## 25 1. Nano- and microfabrication of devices for bacteria

30 Chip devices used for studies of bacteria are in general a few  
centimeters across, a size suitable for manual handling and mount-  
ing onto platforms such as an optical microscope. The topological  
features of these devices can range widely, from the nanometer to  
centimeter scales. The division between nanofabrication and micro-  
fabrication is defined by the highest precision that is demanded for  
35 a device, roughly drawn at  $\sim 100$  nm, the resolution limit of most of

the current optical approaches (see below). The two terms are,  
however, often interchanged since the key principles of fabrication  
are similar and the precision of a particular technique can vary  
according to equipment, recipes, and working conditions. The  
choice of fabrication technique depends not only on the precision,  
5 but also on several other factors such as the chemical and mechan-  
ical properties of the materials. Below, we introduce the basic  
principles of several major classes of fabrication techniques for  
readers who have a background outside nanotechnology.

10 A nano/microstructure is typically fabricated through local  
modification of the chemical or physical properties of a flat  
substrate. The substrate is most commonly prepared through  
depositing a thin layer of organic materials, termed 'resist' onto  
a silicon surface through spin coating. The chemical properties  
of the resist can be modified through patterned exposure to an  
15 energy source (Fig. 1A), which makes a local area either soluble  
or insoluble in a solvent. The photolithography technique  
patterns a surface two-dimensionally by transmitting (typically  
UV) light through a mask to the resist, which is fast and  
relatively inexpensive but requires a pre-patterned mask for  
20 each design. It is well suited for creating features with a  
resolution in the (sub)micrometer to millimeter range, such  
as the 200  $\mu\text{m}$  wide microfluidic channel for studying biofilm  
formation in a constant flow stream<sup>2</sup> depicted in Fig. 1B (panel  
2). Electron-beam lithography uses a local beam of electrons to  
25 draw a custom-designed pattern with, if desired, sub-10 nan-  
ometer resolution. It is required for patterning high-resolution  
features, such as the high-curvature corner of the triangular  
structure shown in Fig. 1B (panel 1), which was used as a mold  
to produce microchambers for shaping a bacterium.<sup>3</sup> After a  
30 quick chemical process that removes either the exposed or  
unexposed resist area, a device now has nano- or microscale  
features, which may be directly used or can be subject to further  
processing such as etching, surface modification, and other  
patterning steps. The structures created by the above methods  
35



**Fabai Wu**

*Fabai Wu obtained his BSc degree in Biotechnology (2008) at Zhejiang University China, his MSc degree in Molecular Bioengineering (2010) at TU Dresden, and his MSc degree cum laude in Nanoscience (2010) at TU Delft. He received his doctoral training from Juan Keymer and Cees Dekker at TU Delft, and is currently finishing his dissertation in the Cees Dekker group. His research focuses on the mechanisms of*

*self-organized pattern formation and chromosome organization in bacteria, and he develops microfluidic tools to study the effect of shape and scale in cell biology.*



**Cees Dekker**

*Cees Dekker received his PhD from the University of Utrecht. Currently, he is Distinguished University Professor at Delft University of Technology, Director of the Kavli Institute of Nanoscience Delft, and KNAW Royal Academy Professor. Trained as a solid-state physicist, he discovered many of the exciting electronic properties of carbon nanotubes in the 1990s. In 2000 he moved to single-molecule*

*biophysics and nanobiology, with research from DNA supercoiling studies of nucleosomes and DNA repair proteins to DNA translocation through nanopores. Recently his research has focused on studying cell division with bacteria on chip, while his ultimate interest is in the direction of realizing synthetic cells.*

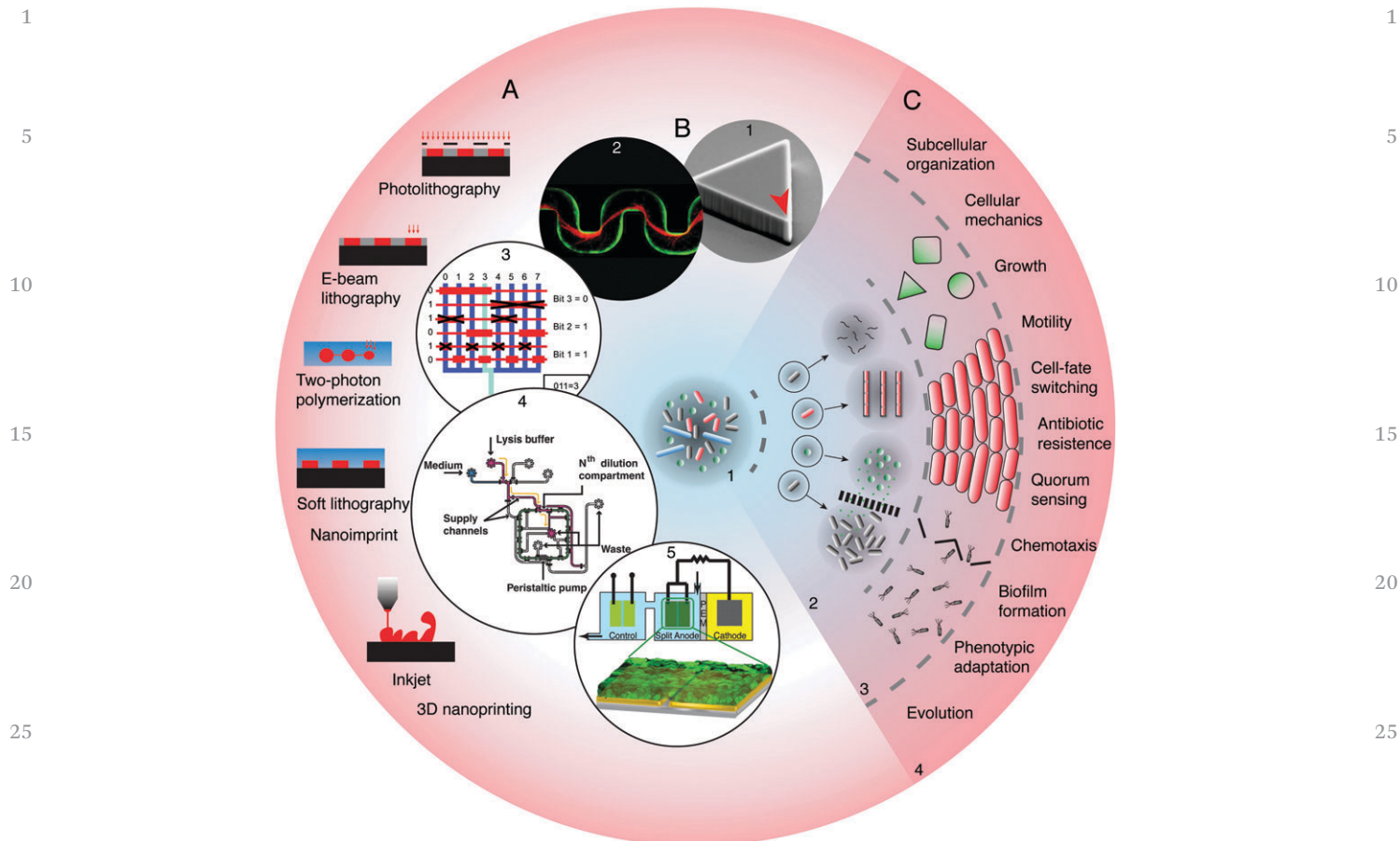


**Fig. 1** Nanofabricated structures and microfluidic devices for bacteria: from techniques to biology. (A) Illustrations of basic nano- and microfabrication processes viewed at cross-sections (left outer circle). Black blocks indicate substrate (mostly silicon). Black lines in the first schematic indicate mask. Grey is spin-coated resist. Red shows the area modified by the lithography techniques. Blue indicates the transparent polymeric material. (B) Images in circles show nano- and microscale structures and their multiplex applications. From top to bottom: (1) a silicon structure with a triangle shape (side lengths 4.5  $\mu\text{m}$ ) nanofabricated through electron-beam lithography (electron-beam steps 20 nm) and etching (red arrow indicates the sharp corner) [adapted with permission from ref. 3]. (2) A 200  $\mu\text{m}$  wide microfluidic channel (fabricated through optical lithography and soft lithography) with fluorescent bacteria forming a biofilm in a flow stream [Reprinted with permission from ref. 2]. (3) Binary inputs defined by pneumatic pumps for large-scale integration of microfluidic devices. [Reprinted with permission from ref. 14]. (4) Schematics of a multiplex microfluidic device used for long-term monitoring of bacteria populations. [Reprinted with permission from ref. 15]. (5) A MEMS device used to measure conductive properties of bacterial biofilms. [Adapted with permission from ref. 16]. (C) Various examples of biological applications in this review. The image illustrates 4 layers divided by dashed lines from left to right: (1) a bacteria community composed of different bacterial species; (2) microstructures spatially separate bacteria for DNA amplification and sequencing, lineage tracking, and chemical communication (from top to bottom); (3) adaptation of bacteria into nanofabricated structures that allow studying cell shape, crowd control, and motility (from top to bottom); and (4) a range of biological questions highlighted in this review.

can be directly transferred to another substrate through direct physical contact, which is used in soft lithography and nanoimprint technologies (Fig. 1A). Both methods uses organic materials that can be molded, hardened, and detached from the original stamp, such that one silicon chip fabricated by a nanoengineer can be used as a reusable mold for a biologist to produce hundreds of devices. In particular, the use of inexpensive, elastic materials such as PDMS (polydimethylsiloxane) and hydrogels in soft lithography<sup>1</sup> paved ways for many applications highlighted in this review. More recently, 3D micropatterning has been developed using two-photon polymerization and inkjet-based 3D printing (Fig. 1A). For studying bacteria, they are particularly useful in creating full confinement and complex topologies.<sup>4,5</sup> Detailed descriptions of the above approaches can be found in ref. 6.

Microfabricated structures can be used to accommodate and manipulate small volumes of fluids, a technology called microfluidics.<sup>1</sup> It can create physical and chemical environments, such as a constant pressure<sup>2</sup> or constant nutrient replenishment,<sup>7</sup> at a level that is inaccessible by conventional laboratory methods. One important function of microfluidics is to create defined chemical gradients, which has for example shed light on the navigation of bacteria through chemotaxis, an application that will not be extensively discussed here given excellent recent reviews by Wessel *et al.*<sup>8</sup> and Rusconi *et al.*<sup>9</sup> Many other applications have been developed. By modulating pressure, multichannel microfluidic devices have been used to switch medium rapidly (see the review by Bennett *et al.*, and references therein<sup>10</sup>). By mixing materials with different properties, a range of structures (microdroplets, microbubbles or microparticles)

1 have been produced that are capable of encapsulating bacteria.<sup>1,11,12</sup>  
 2 By stacking up two layers of PDMS channels, pneumatic valves were  
 3 created that constrict one fluidic channel by applying pressure to  
 4 the adjacent channel.<sup>13</sup> An ingenious development of using the  
 5 opening and closing of such valves as binary inputs has led to large-  
 6 scale complex manipulation using microfluidics<sup>14</sup> (Fig. 1B, panel 3).  
 7 While this review focuses on simple nano- and microstructures for  
 8 studies on bacteria, it is important to realize the strong engineering  
 9 potential of the combination of complex microfluidic circuits and  
 10 synthetic genetic circuits<sup>15</sup> (Fig. 1B, panel 4). Likewise, the combi-  
 11 nation of microstructures and microelectromechanical systems  
 12 (MEMS) can be used to probe various physical properties of bacteria  
 13 as well as their response to electromagnetic, optical and acoustic  
 14 fields that can be generated locally on chips. One important recent  
 15 advance is the studies on the structural origin of the electric  
 16 conductivity of bacterial biofilms<sup>16</sup> (Fig. 1B, panel 5, also see the  
 17 review by Hol *et al.*<sup>17</sup> and references therein).

## 2. Separated affairs

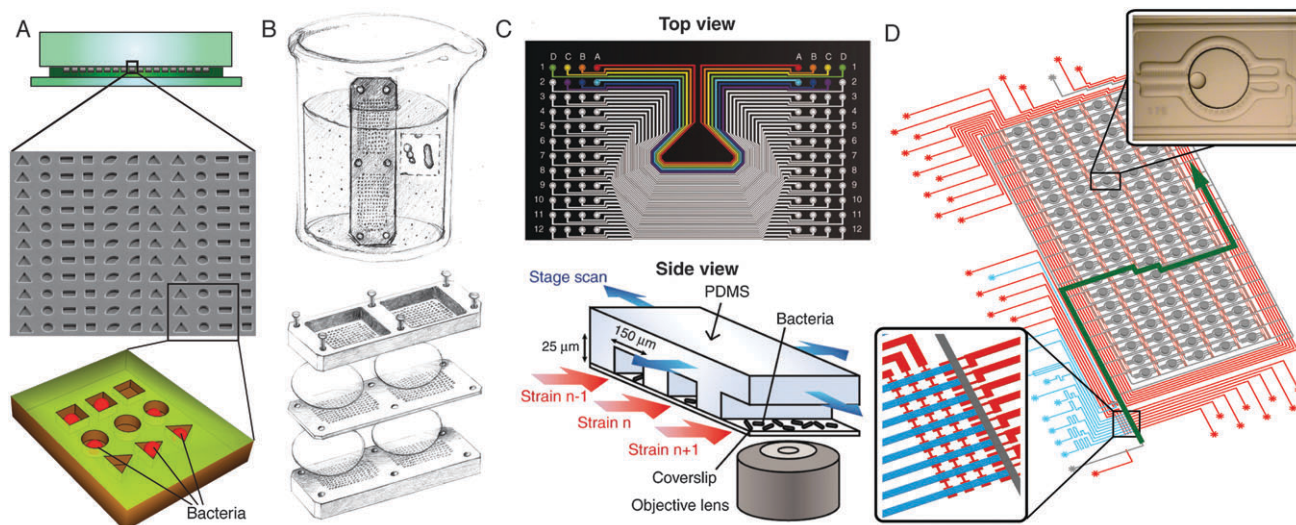
18 Rules in biology are often revealed by observations on individuals,  
 19 and increasingly so, from statistical properties of data gathered  
 20 from ensembles of such observations. Nano- and microfabricated  
 21 devices are perfectly suited for separating individual cells or strains  
 22 for manipulations and downstream analyses.

### 2.1 High-throughput platforms

23 Microstructures offer the capabilities to confine any small  
 24 amounts of bacterial culture, encompassing volumes as small

25 as one single cell. A large array composed of say  $10^5$  micro-  
 26 chambers can for example be fabricated in an area of only a few  
 27 square millimeters, spatially separating bacteria for subsequent  
 28 manipulation and detection (Fig. 2A). This feature makes micro-  
 29 structures particularly effective as high-throughput platforms.

30 Diverse approaches have been developed to separate and  
 31 encapsulate bacteria. The simplest forms are microchamber  
 32 arrays from the hydrogel, PDMS, or plastic, made mostly  
 33 through soft lithography (Fig. 2A). These are often filled with  
 34 bacteria by simple inoculation of bulk culture before getting  
 35 sealed by the hydrogel, a semipermeable membrane, or a piece  
 36 of coverglass. These simple devices do not necessarily involve  
 37 microfluidic circuits and can be readily adopted by regular  
 38 microbiology laboratories, which can obtain microfabricated  
 39 molds with the desired patterns commercially. Takeuchi  
 40 *et al.*,<sup>18</sup> Renner *et al.*,<sup>19</sup> and Wu *et al.*,<sup>3</sup> for example, pipetted a  
 41 small volume ( $\sim 1 \mu\text{l}$ ) of bacterial culture onto the surface  
 42 patterned with microchambers, where bacteria were distributed  
 43 into the chambers by capillary force after the surplus liquid was  
 44 absorbed by agarose (Fig. 2A). This approach takes advantage of  
 45 the large number of microchambers: while bacterial cells enter  
 46 the microchambers stochastically, the chambers with a desir-  
 47 able inoculation density can be selected afterwards through  
 48 automated data analysis. The throughput for specific applica-  
 49 tions can be optimized by tuning the volume and density of the  
 50 inoculated bacterial cultures as well as the size and distance of  
 51 the microchambers. Such an approach has been used to study  
 52 cellular mechanics, cell growth, cell division and subcellular  
 53 organization, which are described in Section 3.3.



54 Fig. 2 High-throughput devices made from nano/microfabricated structures. (A) A simple device using PDMS microstructures of different shapes to  
 55 confine single bacterial cells. Shown from top to bottom are a schematic of the cross section of the agarose/PDMS/glass sandwich, a scanning electron  
 56 microscopy image of the microstructures, and an illustration of bacteria in these microchambers. [Adapted with permission from ref. 3]. (B) Sketches of  
 57 the 'iChip' used to capture single bacterial cells from a soil suspension (top) and the through-holes sandwiched by semipermeable membranes (bottom)  
 58 for further cultivation. [Reprinted with permission from ref. 21]. This device enabled culturing of unculturable microbes and led to the discovery of new  
 59 antibiotics [ref. 22]. (C) A microfluidic device with an array of microfluidic channels used for high-throughput quantification of the proteome and  
 60 transcriptome of single bacteria through fluorescence imaging. [Reprinted with permission from ref. 23]. (D) A programmable microfluidic device  
 61 composed of peristaltic pumps (magnified at the bottom left) and droplets (magnified at top right) for enclosing single bacteria for cultivation and  
 62 genome sequencing. The green arrow shows one possible flow path. [Adapted with permission from ref. 12].

1 The importance of physically separating bacteria into inde- 1  
pendent compartments is prominently exemplified by efforts to  
culture bacteria from natural microbial communities. This  
overcomes a long-standing issue that the majority of micro-  
5 organisms are not cultivable on a conventional Petri dish, as a  
'winner-takes-all' competition leads to overgrowth of fast-  
growing bacterial species.<sup>20,21</sup> Nichols *et al.* developed a device  
called 'isolation chip' (or 'iChip'), which contains millimeter-  
sized through-holes for isolating bacteria from the natural  
10 environment and cultivating the species that were otherwise  
uncultivable<sup>21,22</sup> (Fig. 2B). The iChip, made from (commercially  
manufactured) polyoxymethylene, was dipped into a liquid  
suspension of soil samples for encapsulation of single micro-  
bial cells into the through-holes, and then sandwiched by  
15 semipermeable polycarbonate membranes that allow chemical  
exchange of the enclosed colonies with the environment and  
with each other. The principles and advantages of semiperme-  
able membranes are further discussed in Section 2.3. This  
technique allows microbes from the soil sample to grow in  
20 separated spaces into millimeter-sized colonies (allowed by the  
chamber size) ready for downstream isolation and analysis.  
This technique provides a high-throughput platform for culti-  
vating numerous new species that cannot be cultivated inde-  
pendently. In contrast to a ~1% successful cultivation using  
25 Petri dishes, iChip was reported to recover up to 50% of the  
species,<sup>21</sup> which is a spectacular advance. By screening the  
potential application of the metabolic compounds produced by  
the bacteria cultivated using iChip, Ling *et al.* recently discov-  
ered a novel antibiotic that effectively kills persistent pathogens  
30 such as *Staphylococcus aureus* or *Mycobacterium tuberculosis*, so  
far without raising antibiotic resistance.<sup>22</sup>

Independent culturing of bacteria in separated compart-  
ments allows high-throughput analyses of different strains  
and culturing conditions. A microfluidic device is most com-  
35 monly constructed by covalently bonding a PDMS chip and a  
piece of glass, enabled by a simple oxygen plasma treatment  
(Fig. 2C). Using a PDMS-based microfluidic device as simple as  
smartly stacking up 96 parallel channels, Taniguchi *et al.*  
injected individual bacterial strains into individual channels  
40 such that 96 different strains can be imaged simultaneously<sup>23</sup>  
(Fig. 2C). Here, each strain has a different gene fused to a yellow  
fluorescent protein gene. This approach facilitated the quanti-  
tative imaging of in total 1018 strains, leading to a quantifica-  
tion of the proteome and transcriptome in single cells with  
45 single-molecule sensitivity. Among other essential quantitative  
findings, they showed that proteins of single cells and mRNA  
copy numbers for any given gene are uncorrelated,<sup>23</sup> contrast-  
ing the conventional perception that protein abundance scales  
with mRNA abundance. A key design principle of this study was  
50 to use semi-automation that reduces an unmanageably abun-  
dant sampling task to a feasible operation. In this case, in each  
experiment, all 96 microfluidic channels had to be manually  
connected to tubing for injection of bacteria, but it made  
downstream microscopy and analyses significantly more effi-  
55 cient. This indicates that, while microfluidics has the promise  
of complex manipulations that potentially automate many

processes, adopting a single feature at a time can already lead 1  
to an enormous advantage for a conventional microbiology lab.

Microfluidic devices can be much more versatile in single-  
cell analysis when integrating valve and droplet technologies,  
5 as they enable real-time compartmentalization and complex  
spatio-temporal control.<sup>1,11-15</sup> Eun *et al.* encapsulated single  
bacterial cells in agarose microparticles with volumes compa-  
tible with fluorescence-activated cell sorting (FACS).<sup>11</sup> Such a  
platform enabled high-throughput screening and sorting of  
10 bacterial phenotypes in different chemical environments, such  
as the emergence of antibiotic resistance, for subsequent  
genotypic analysis.<sup>11</sup> Combining both pneumatic valves and  
microdroplets, Leung *et al.* built a programmable, multiplex  
microfluidic device capable of precisely sorting, analyzing and  
15 cultivating microbes at the single-cell level<sup>12</sup> (Fig. 2D). This  
device used peristaltic pumps to dispense a sub-femtoliter  
volume droplet of reagent or cell culture (from one of 8 inlets)  
into a flow stream, delivering it into one of the 95 storage  
chambers by using microvalves. Through an elegant control of  
20 the flow rate, the droplet can either be docked at the entrance  
of the chambers for merging with another incoming droplet, or  
flushed away for downstream analyses. In addition, a cell-  
sorting module was integrated upstream through a feedback  
mechanism between optical detection and pumping, and an  
25 elution process is implemented downstream to recover the  
samples for off-chip analyses. The authors multi-purposed this  
droplet-based microfluidic device for various high-throughput  
applications including bacterial cell sorting and cultivation,  
taxonomic gene identification, and single-cell whole-genome  
30 sequencing.<sup>12</sup>

## 2.2 Tracking lineage

In changing environments, a bacterial cell is constantly chal-  
lenged with decisions to switch on and off the expression of  
genetic modules that define its metabolic capacity (*e.g.* through  
35 enzymes and transporters) or the life style (*e.g.* through motility  
and biofilm formation). It is increasingly clear that the pheno-  
types of bacterial cells can vary even in the same environment,  
and can switch (seemingly) stochastically without environmen-  
tal cues (see Norman *et al.* and references therein<sup>24</sup>). Micro-  
40 structures can offer spatial separation of populations and allow  
tracking of individual lineages over time in a steady chemical  
environment<sup>7,24-29</sup> (Fig. 3A-D). Through inter- and intra-  
lineage comparisons of phenotypes made possible by this  
approach, biologists are starting to understand the origins  
45 and consequences of phenotypic variations (Fig. 3E). While  
bacteria have developed mechanisms to damp undesirable  
variations in order to reach homeostasis<sup>28,29</sup> (Fig. 3F), other  
variations are now known to be beneficial as a bet-hedging  
strategy, that is, a stochastic switching of the phenotype for  
50 adaptation to different environments<sup>24,27,30</sup> (Fig. 3G and H). In  
addition, long-term tracking of lineage revealed the temporal  
control by genetic circuits responsible for oscillatory behav-  
iors<sup>26</sup> (Fig. 3I), and cell-fate decisions<sup>24</sup> (Fig. 3G).

The main challenge for tracking a large number of lineages 55  
is that each single exponentially growing population rapidly



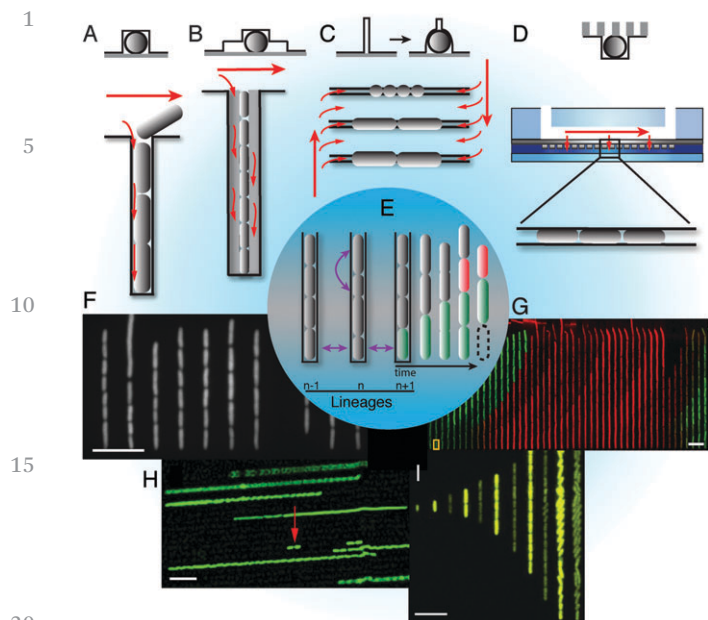


**Fig. 3** Line channels for lineage tracking. (A–D) Schematics of various line-channel devices with different nutrient accessibilities. (In each panel: top is cross-section and bottom is top view). Large red arrows show the direction of the fluid flow; small red arrows show nutrients accessing the channels with cells. (E) Illustration in the center: linear colonies in the line channels are used for inter-lineage (numbered  $n - 1$ ,  $n$ ,  $n + 1$ ) and intra-lineage (e.g. in lineage  $n$ ) comparisons (magenta arrows), and for long-term tracking allowing studies of cell-fate switching (from grey to red cell) and the mechanisms of growth (green), cell size control, and cell death (dashed rod). (F–I) Fluorescent images of cells growing in line channels. (F) A snap shot of *E. coli* lineages growing in the mother machine. [Reprinted with permission from ref. 7]. (G) A kymograph of a *B. subtilis* lineage. Green, the motile state; red, the chained state; yellow box, time point of cell-fate switching. The time interval between frames is 10 min. [Reprinted with permission from ref. 24]. (H) A snap shot of *E. coli* cells growing in line channels. The red arrow indicates two cells showing slow growth. [Reprinted with permission from ref. 30]. (I) Time-lapse images showing Cyanobacteria *Synechococcus elongatus* with YFP expression under the promoter of *kaiBC* genes, which are involved in controlling circadian oscillations. The time interval between frames is 12 h. [Reprinted with permission from ref. 26]. Scale bars in F–I are all 10  $\mu\text{m}$ .

expands to a size that is unsuitable for recording and analysis. An elegant alternative was the development of a microfluidic device dubbed the ‘mother machine’, which was composed of hundreds of line channels each sized to such a small width that they could only accommodate a single row of bacteria<sup>7</sup> (Fig. 3A). These lines were connected to a large flow trench, which replenished the nutrients through diffusion as well as removed cells that exited the line channels. As a result, the features of the mother cell that continuously remained at the end of a line channel and many newborn daughter cells could be recorded over time (Fig. 3F). The number of generations tracked per lineage was, however, limited due to the distance constrained by nutrient diffusion. Norman *et al.* added a shallow side channel to enable feeding over a longer length scale for studying *B. subtilis*<sup>24</sup> (Fig. 3B); this feature is yet to be tested for Gram-negative bacteria since they can potentially squeeze into

the shallow side channels when crowded.<sup>31</sup> The use of agarose can allow for much more efficient diffusion of nutrients over a long distance (over 100  $\mu\text{m}$  from the feeding channels)<sup>25,26</sup> (Fig. 3C). However, agarose is less stiff and thus less effective in confining the cells strictly in a row<sup>26</sup> (Fig. 3I). Moffitt *et al.* solved this issue by fabricating lines that were narrower (0.3–0.8  $\mu\text{m}$ ) but deeper (1–1.5  $\mu\text{m}$ ) than the width of the bacteria ( $\sim 0.9 \mu\text{m}$  for *E. coli*), such that the bacteria slightly pushed the agarose aside during its growth along the linear tracks<sup>25</sup> (Fig. 3C). The efficient diffusion in agarose also entails an efficient exchange of signaling molecules and metabolites between lineages,<sup>25</sup> which can be advantageous or disadvantageous depending on specific applications. Furthermore, a channel-length-independent delivery of nutrients and drugs can be achieved by vertical diffusion through a semi-permeable membrane,<sup>30</sup> which in principle can allow for tracking of lineages for a large number of generations (Fig. 3D). Besides differences in stiffness, different materials also have different refractive indices and transparencies that can affect detection of bacteria in line structures using light microscopy.<sup>32</sup>

Lineage tracking revealed the robustness of cell growth, division, and size control. Wang *et al.* grew *E. coli* cells in the ‘mother machine’ for hundreds of generations, and found that the growth rate of *E. coli* cells was strikingly constant even in the mother cells that invariably inherited the old pole after each cell division<sup>7</sup> (Fig. 3B and F). While the inheritance of old pole had previously been proposed to lead to ageing as it inherit old cell wall material and misfolded proteins that aggregate at the polar regions, such ageing did not have a noticeable effect on the growth rate. By using the ‘mother machine’, the authors were able to maintain a steady-state growth of bacteria much better than previous studies using an agar pad (see Wang *et al.*<sup>7</sup> and references therein). They showed that aging, while not affecting the growth rate, did lead to an increase in cell damage, which was indicated by the increasing rate of filamentous growth and cell death.<sup>7</sup> Using a similar experimental approach, Taheri-Araghi *et al.* quantified the sizes of cells over many generations of growth and found that for both *E. coli* and *B. subtilis*, cells added a constant volume in between two division cycles, irrespective of their original sizes.<sup>29</sup> By abiding to this principle of constant cell-size extension, these bacteria reduce cell-size variations in steady-state growth and reach cell-size homeostasis. These findings were also reported for *Caulobacter crescentus* and *E. coli* by Campos *et al.* using alternative microfluidic devices, where more cells were cultivated in each chamber, with lineage tracking aided by computer programs.<sup>28</sup>

Lineage tracking has greatly elucidated the nature of environment-independent phenotypic variations and cell-fate switching. In a fast-growing culture, a small subpopulation of cells at a slow-growing state was found to be responsible for bacterial persistence to antibiotic treatments, and a mutation in the gene *hipA* increased the fraction of slow-growing cells significantly enhanced persistence<sup>30</sup> (Fig. 3D and H). Recently, another study showed that persistence could also be caused by an infrequent pulsing in the expression pattern of the proteins (KatG in *Mycobacterium smegmatis*) that are responsible for activating the antibiotics (INH), unrelated to growth rate.<sup>27</sup>

The authors proposed that stochastic switching of phenotype can be a universal strategy that enables adaptation to a broad spectrum of stress types, in addition to the costly sensing systems that respond to specific types of stress.<sup>27</sup> Although often stochastic switching of phenotype can be understood through the fluctuations inherent to the chemical environment inside of the cells,<sup>23</sup> recent studies start to show that pulsing can be a regulatory feature hardwired in the genetic circuits (see review by Levine *et al.*<sup>33</sup>). Norman *et al.* studied the switching between the motile and chained states in *B. subtilis*, and found that although the emergence of the chained, multicellular state was infrequent, the time spent at the state was tightly controlled<sup>24</sup> (Fig. 3C and I).

### 2.3 Physical separation and chemical communication

Bacteria are social creatures. They communicate through secreting and sensing signaling molecules, cooperate to endure stress, and benefit from each other's unique metabolic capacity. They also combat for resources, and prey on one another. A great challenge in dissecting the social interactions between bacteria in bulk is to distinguish whether they are of a chemical or physical nature. Microstructures, when implemented with elements such as semipermeable membranes, hydrogels, and nanoslits, can be used to physically separate bacterial species or lineages while allowing chemical communications between them (see the schematics in Fig. 4).

Members of a natural bacterial community often exhibit inter-dependent metabolic activities, that is, the growth of one species relies on metabolites secreted by another species. Thus, for example, the chemical exchange enabled by the co-culturing process based on iChip (introduced in Section 2.1) facilitated culturing of uncultivable species.<sup>21</sup> However, the complexity of metabolic exchange processes has only started to be dissected.

Kim *et al.* constructed a microfluidic device where 3 bacterial species were inoculated into spatially separated microwells, which were all connected to the same channel that mediates chemical communications<sup>20</sup> (Fig. 4A). These 3 species were respectively responsible for supplying the nitrogen source, carbon source, and for degrading antibiotics. They found that these species coexisted well with a finite inter-chamber distance, while the community collapsed either without any physical separation or with distances too large for the resources to be shared through diffusion.<sup>20</sup> Thus, the authors demonstrated that dynamic microbial communities should be understood in the context of spatial structures, which enable spatially separated growth and dictate the diffusivity of metabolic compounds. Recently developed 3D-printing of hydrogel structures provided even more versatile platforms to enclose and spatially organize multiple populations of bacteria for engineering of bacterial communities.<sup>5</sup>

Bacteria make collective decisions through quorum sensing. Quorum sensing was discovered as a cell-density-dependent signaling behavior. By confining single bacteria in small hydrogel chambers that were chemically isolated, quorum response was triggered by accumulated quorum-sensing molecules within the chambers despite the low cell density.<sup>34,35</sup> These experiments underlined the importance of understanding chemical communications within the context of spatial structures. Flickinger *et al.* used hydrogels to physically separate bacterial biofilms and found that quorum sensing through the hydrogel chamber walls stimulated cell growth within the biofilms (Fig. 4B).<sup>36</sup> The well-understood circuit responsible for quorum sensing was successfully applied to engineer synchronous cell behaviors. Prindle *et al.* constructed liquid crystal display like arrays of microchambers hosting independently growing bacterial colonies that detect arsenic.<sup>37</sup> They coupled

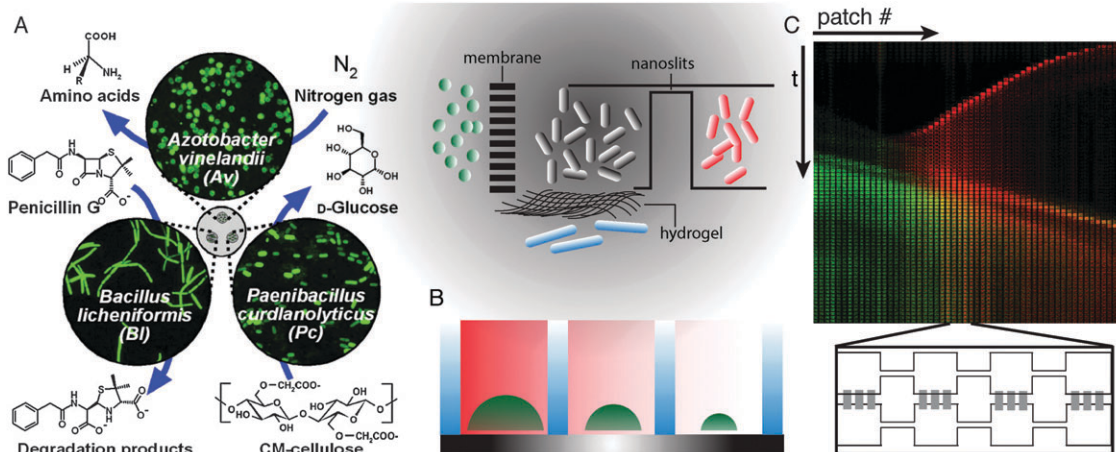


**Fig. 4** Chemical communication between physically separated bacterial populations in microstructures. A schematic in the top-middle shows bacteria spatially separated by a semipermeable membrane, hydrogel or nanoslits. (A) Three bacterial species sharing metabolic products and penicillinase through a chemical chamber that mutually separates the bacteria through a cellulose membrane. [Reprinted with permission from ref. 20]. (B) Hydrogel walls (blue) separating bacterial biofilms (green), which communicate through quorum sensing molecules HSL (red) that promote biofilm growth. [Modified from ref. 36]. (C). Kymograph showing two populations of the same *E. coli* strain travelling in two parallel microhabitat patches that are chemically connected through 200 nm deep nanoslits (see the bottom illustration, nanoslits in grey). The two populations enter from the left (green) and right (red), respectively, and influenced each other's propagation although they do not have physical contact. [Reprinted with permission from ref. 38].

1 the behavior within the bacterial colony through quorum sensing, which is then coupled between physically separated colonies through rapid gas-phase redox signaling that penetrates through the PDMS material. These bacteria synchronized their  
5 frequency of fluorescence oscillations over a large scale, showing the potential for constructing low-cost genetic biosensors.<sup>37</sup>

Bacteria were found to mark territory through signaling without physical interactions. Van Vliet *et al.* harvested bacteria from the same exponentially growing culture in a shaking tube and separately inoculated them into inlets at distant ends of two separate centimeter-long habitats, each containing many chambers that were mutually connected by thin corridors<sup>38</sup> (Fig. 4C). These two parallel habitats were connected through nanoslits that are 200 nm in height, too small for *E. coli*  
10 bacteria to swim through, but large enough to allow for chemical coupling. As shown in Fig. 4C, the traveling front of one population (indicated in red) stopped progressing forward after it met the travelling front of the other population (labeled in green). Thus, this study elegantly demonstrated that the  
15 population fronts collided upon chemical communications alone without physical interactions.<sup>38</sup>

### 3. Decoding geometries

25 Bacteria live in a world of structured environments. Nano- and microfabrication can achieve systematic control over the global as well as local topological features of the microenvironment, and thus can unravel the effects of the boundary geometry for  
30 bacterial population and even at the level of subcellular organization.

#### 3.1 Populating a topological space

35 The topological features of natural habitats of bacteria influence the diffusivity of signals, nutrients, and metabolic waste, which are essential triggers of growth, attachment, and motility – behaviors that are in turn constrained by space. Hence, it is essential to understand the physiology and behavior of bacteria in the context of their spatial environment (Fig. 5).

40 Discreteness and heterogeneity are prominent features that distinguish the natural habitats of bacteria from well-mixed liquid cultures in the laboratory. Various forms of microhabitats have been fabricated to explore the effects of spatial heterogeneity on the ecological and evolutionary properties of bacterial populations.  
45 Park *et al.* loaded *E. coli* cells into a microfabricated maze, where instead of dispersing throughout, bacteria formed travelling waves that nucleated dense populations into several dead ends within the maze<sup>39</sup> (Fig. 5A). This self-organized clustering phenomenon was further demonstrated in a more defined structure, and was  
50 found to be induced by the sensing of self-secreted amino acids by chemotactic receptors.<sup>39</sup> The authors thus showed that chemotaxis is not only employed by the cells to sense the gradient of exogenous nutrients as commonly understood, but also utilized to gather individuals to collectively seek for *e.g.* microcavities, a  
55 strategy that is likely beneficial for surviving nutrient deprivation.<sup>39</sup> Constructing a linear array of microhabitat patches connected by

thin corridors, Keymer *et al.* observed the formation of a metapopulation, that is, subpopulations coexisting in different patches and interacting through local extinction and colonization<sup>40</sup> (Fig. 5B). They further showed that if nutrients and oxygen were supplied heterogeneously throughout the MHPs, such a metapopulation showed a rapid invasion from the high-resource areas to low-resource areas, revealing that the emergence of heterogeneous population structures facilitated by structured space can benefit adaptation.<sup>40</sup> The adaptive advantage of a metapopulation in a structured environment was further exemplified by a report of an accelerated emergence of antibiotic resistance in a large hexagonal device composed of 1200 hexagonal wells that were interconnected through corridors.<sup>41</sup>

Local geometric features can affect the population structure at the global scale. Corridors between ecological niches, for example, can constrain the connectivity between these niches, both chemically and physically (Fig. 5C). Hol *et al.* constructed a simple artificial ecosystem with a narrow corridor of 100  $\mu\text{m}$  in length connecting two large habitats that were both constantly replenished with nutrient (Losogeny broth medium) but only one of the two habitats with an antibiotic kanamycin at a lethal concentration<sup>42</sup> (Fig. 5D). The corridor created a diffusion barrier that renders a steep concentration gradient at the interface between the two habitats, where bacteria combated to survive under antibiotic stress. The authors found that a dense population of bacteria from the antibiotic-free zone was able to invade and colonize the antibiotic zone within several hours. Here, a sufficiently high density of the invading population was critical. As genetic mutations were not found at least in the first 29 hours after invasion, the authors provided evidence that the phenotypic adaptation responsible for the initial niche invasion can facilitate establishing a sizeable population as basis for the emergence of heritable genetic change.<sup>42</sup>

Corridors also interfere with the behavior of swimming bacteria through physical collisions, where their geometric features can affect population-scale distributions. As shown in Fig. 5E, Galajda *et al.* used a series of funnel walls that bias the destination of otherwise randomly moving *E. coli* towards one side of the device<sup>43</sup> (for follow-up applications of funnels, see the review by Rusconi *et al.* and references therein<sup>9</sup>).

#### 3.2 Crowded and confined

At a critical scale where space becomes the constraining factor for the colonization by bacteria, the physical interactions between bacteria and the spatial boundary of the environment start to play an important role. Such a scenario occurs in the overgrowth with high-nutrient conditions, in the formation of biofilms, or by the self-organized clustering into tiny cavities that was mentioned above. How do bacteria organize themselves in these various forms of super-structures? Cho *et al.* inoculated rod-shape *E. coli* cells in chambers with various distinct shapes, which were connected to fluidic channels that replenished nutrients and flushed away escaped cells.<sup>44</sup> In these chambers, bacteria showed orientation, growth and collective motion according to the shapes of the chambers and their locations within the chambers<sup>44</sup> (Fig. 5F). The authors

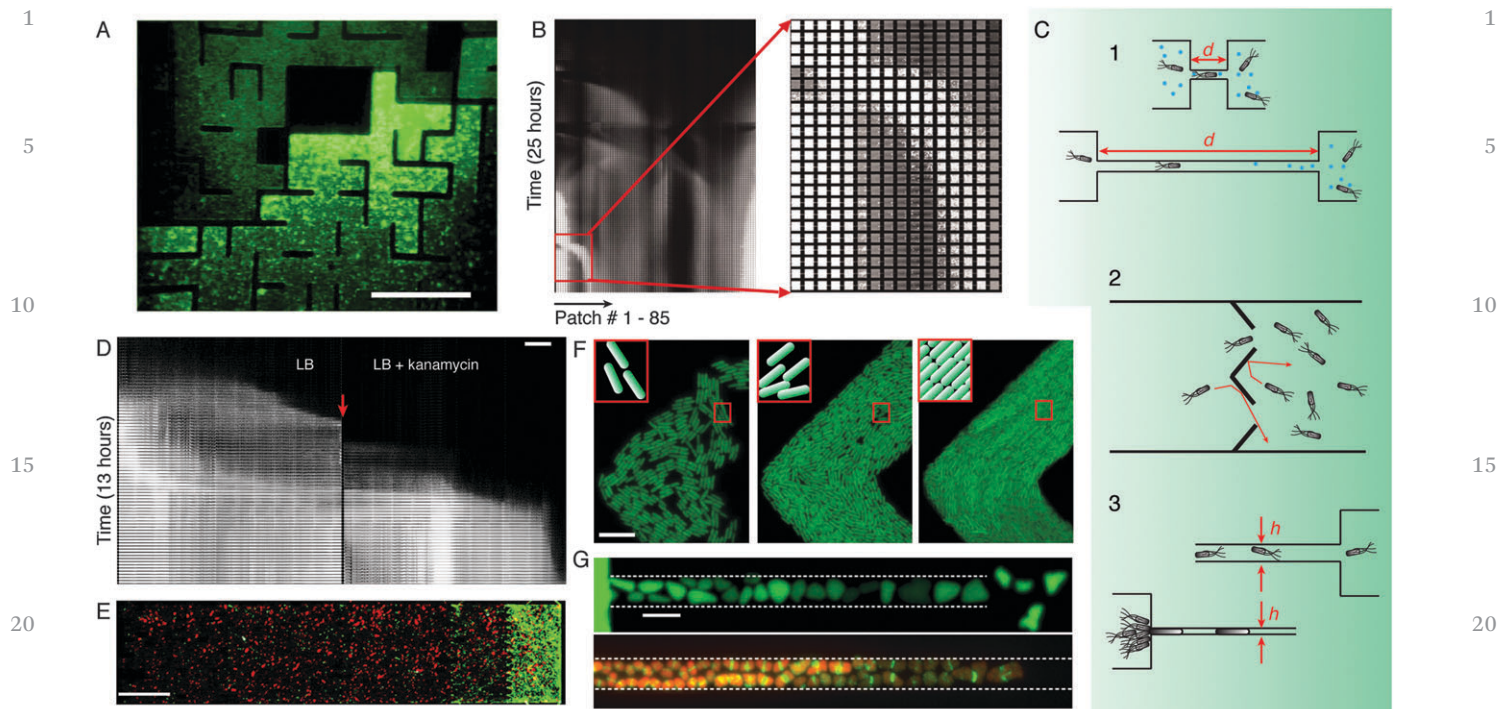


**Fig. 5** Effect of nanofabricated topological features on bacterial populations. (A) Chemotactic *E. coli* bacteria (with green fluorescence) cluster at dead ends of nanofabricated mazes. Scale bar, 200  $\mu\text{m}$ . [Reprinted with permission from ref. 39]. (B) Temporal evolution of a bacterial metapopulation in 85 microhabitat patches connected through narrow corridors. [Reprinted with permission from ref. 40]. (C) Illustrations showing how the geometries of the corridors between microhabitats affect the behavior of bacteria. 1. The length ( $d$ ) of the corridors affects the diffusivity of the nutrients, antibiotics, and signaling molecules (depicted by the blue circles) between two chambers, thus reducing chemical communication (as in D). 2. Funnels concentrate bacteria to one side (as in E). Red indicates the paths of the swimming bacteria before and after collision onto the funnel walls. 3. Decreasing the width ( $h$ ) of the corridors to smaller than the cells stop them from swimming through (top), but instead cause the Gram-negative bacteria to grow and squeeze through (bottom) (as in G). (D) A dense population of fluorescent *E. coli* bacteria invading a new territory with a lethal concentration of kanamycin. The corridor between the left and right device, indicated by the red arrow, is 100  $\mu\text{m}$  long and 5  $\mu\text{m}$  wide. Scale bar, 1 mm. [Reprinted with permission from ref. 42]. (E) Motile *E. coli* (in green) are concentrated by a series of funnels (shown in the illustration at the right) to the rightmost chamber, while the non-motile *E. coli* (in red) homogeneously distribute throughout the device. Scale bar, 200  $\mu\text{m}$ . [Reprinted with permission from ref. 43]. (F) With increasing cell density, bacteria self-organize to orient themselves according to their location in the chambers with a defined geometry. Time intervals between frames are 2 h and 22 h, respectively. Top left corners zoom in on the bacteria in the red rectangles indicated at the right. Scale bar, 10  $\mu\text{m}$ . [Adapted with permission from ref. 44]. (G) *E. coli* bacteria squeeze through channels 300 nm in depth and changed their lateral dimensions and shapes (top view). The boundaries of the shallow channels are indicated by dashed lines. Top panel shows cytosolic fluorescence [Reprinted with permission from ref. 31]; bottom panel shows chromosome (red) and division machinery (green) [Image courtesy of Jaan Männik (ref. 46)]. Scale bar, 5  $\mu\text{m}$ .

used computer simulations to show that such self-organization phenomena can be explained by the combined effect of cell shape and mechanical forces between cells. Moreover, the resulting cell arrangements can decrease the mechanical stress induced by cell growth and promote efficient diffusion of nutrients.<sup>44</sup> Bacteria find solutions to crowding not only through minimizing mechanical stress, but also through maximizing attachment to local surface structures. This was exemplified by the spontaneous ordering of bacterial cells within periodically arranged nanoposts<sup>45</sup> (see Hol *et al.* for more examples of surface adhesion<sup>17</sup>). The effect of crowding on the physiology of bacteria is largely unclear. In a first study, Connell *et al.* used hydrogel structures polymerized through multiphoton lithography to trap bacteria, and found that bacteria at high densities showed a much higher tolerance to the antibiotic gentamycin.<sup>4</sup>

Invading new territories is another solution to local crowding that can tremendously benefit the survival of a population

or a species. Männik *et al.* used nanofabrication to systematically decrease the corridor between a patch that was highly populated by bacteria and an empty patch replenished with nutrients. For wide corridors, the bacteria would, not surprisingly, swim to the well-resourced empty patch. For very small corridors, however, they found a surprising effect: Here, rod-shape *E. coli*, Gram-negative bacterial species, were able to squeeze themselves through corridors (made as slits in the silicon material) that were much narrower than their natural diameter of  $\sim 1 \mu\text{m}$  and subsequently propagate by growth<sup>31</sup> (Fig. 5G). The ability for bacteria to penetrate dimensions smaller than their size appears to depend on the internal turgor and the stiffness of the cell wall, as Gram-positive bacteria *Bacillus subtilis* did not manage to do so to the same extent.<sup>31</sup> *E. coli* cells were found to adopt pancake-like irregular shapes while squeezing through shallow channels that were made for imaging<sup>31</sup> (Fig. 5G). These cells, although large and irregular in shape, can still partition their cytosolic volumes and DNA

content equally into daughter cells during cell division<sup>46</sup> (Fig. 5G). It is an intriguing question whether and how other machineries within the bacteria respond to changes in the cell shape.

### 3.3 Cell-shape sculpting

Zooming in on the inner environment of a cell, the spatial organization of intracellular molecular networks is dictated by the shape and size of the cell boundary. While the general importance of the cell shape in bacteria is increasingly appreciated, it has been difficult to systematically probe the effects of specific geometric features embedded in the cell shape. Microstructures can be used to impose a certain shape to single bacteria. The ability to manipulate the cell shape of bacteria using nanofabricated structures is now starting to unravel the interplay between cell boundary and the molecular networks therein.<sup>3,18,19,31,46,47</sup>

The use of microstructures to guide the growth of single bacteria was first elegantly demonstrated by Takeuchi *et al.*<sup>18</sup> As shown in Fig. 6A, single *E. coli* bacteria were inoculated into donut-shaped microwells several microns in depth made from agarose supplemented with nutrients and a division-inhibitor cephalaxin. After several hours, the growth of the bacteria followed the curvature of the microwells, yielding filaments that curled up along the defined shape of the agarose walls. Interestingly, after being released from the chambers, the cells maintained the spiral shapes, and adopted various modes of swimming patterns depending on the helicity of their cell shapes. Cabeen *et al.* found that the mode of growth imposed

by the agarose wells was similar to the emergence of the crescent shape of *C. crescentus*, leading them to propose that it is the mechanical strain borne by the cytoskeleton crescentin filaments anisotropically alters the cell-wall-insertion kinetics to produce curved growth.<sup>47</sup>

Realizing that spatial constraints can mechanically shape bacterial growth opened up a range of possibilities for tackling timely questions in cell biology (Fig. 6B). For example, proteins and lipids were found to localize to the cell poles of bacteria by sensing the negative curvature (see Weibel *et al.* and references therein<sup>19</sup>), and dynamic protein patterns self-organize to form spatial gradients along the long axis of the cell (see Wu *et al.* and references therein<sup>3</sup>).

Renner *et al.* generated cell-wall-less spheroplasts that were highly moldable.<sup>19</sup> Long filamentous bacteria were osmotically protected by sucrose and treated with lysozyme before inoculating into agarose chambers. Without a stiff cell wall, these spheroplasts easily adapted to the shapes of the elliptical chambers with different aspect ratios and polar curvatures (Fig. 6C). The author stained the cells with nonyl acridine orange (NAO), a fluorophore that has high affinity for anionic lipids such as cardiolipin, and found that the labeled lipid microdomains preferably localize at the cell membrane area with high negative curvature (Fig. 6C). Some proteins however had lost their dynamic localization patterns in these spheroplasts, suggesting that the experimental protocols were yet to be improved to maintain the viability of the cells.

Improving upon the above methods, Wu *et al.* combined the confinement strategy using nanofabricated chambers with a

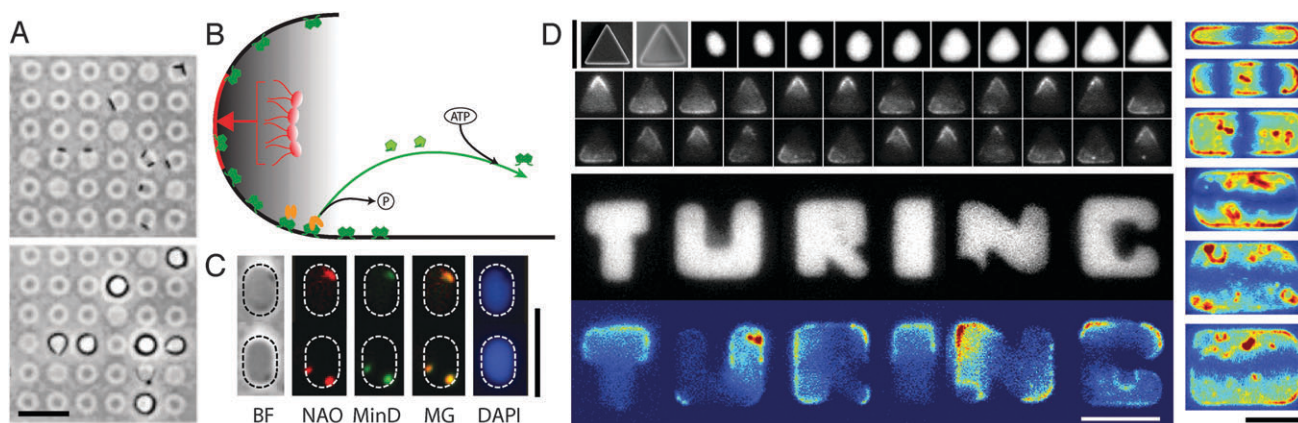


Fig. 6 Cell shaping techniques used to study subcellular organization. (A) Rod-shape *E. coli* (top) grow into filaments (bottom) as they adapt to the curvature of the donut-shaped agarose chambers. Scale bar, 20  $\mu\text{m}$ . [Reprinted with permission from ref. 18]. (B) A schematic that illustrates the mechanisms responsible for the polar localization of proteins and lipids. The curved line at the left depicts the bacterial cell pole and the flat line at the bottom depicts the non-polar membrane. Anionic lipids (shown in red) preferably form microdomains that have an intrinsic curvature and thus prefer the negatively curved cell pole. MinD proteins (in green) oscillate between the two cell poles through a reaction-diffusion mechanism. When MinE (orange) binds to the membrane-bound MinD (green), it triggers the ATPase activity of MinD and unbinds the latter from the membrane. MinD.ADP diffuses in the cytosol while undergoing an ADP-ATP exchange cycle and relocate at a distance (green arrow). (C) Spheroplasts of *E. coli* cells prepared using lysozyme adopt the shapes of microchambers with an elliptic shape. BF, bright field; NAO, nonyl acridine orange signal; MinD, YFP-MinD signal; MG, merge; DAPI, a DNA stain. Scale bar, 5  $\mu\text{m}$ . [Reprinted with permission from ref. 19]. (D) The 'Cell-sculpting' method used to shape bacteria into defined shapes, in which Min proteins oscillate. Top left: SEM images of the silicon mode and the PDMS structure followed by time-lapse fluorescence images of slow cell growth into a triangle shape in the PDMS structure (top row), followed by time-lapse fluorescence images of GFP-MinD oscillations in the shaped cells. Bottom left: A snapshot of cytosolic fluorescence (in grey scale) and GFP-MinD fluorescence (in color map) of six individual bacteria that were shaped into the letters 'TURING'. Right: Standard-deviation images of GFP-MinD patterns in rectangular 9  $\mu\text{m}$  long cells with cell widths increasing from 1 to 6  $\mu\text{m}$ . Color maps: values from high to low: red-yellow-green-blue. Scale bars are all 5  $\mu\text{m}$ . [Reprinted with permission from ref. 3].

1 milder treatment that alters the cell wall synthesis. In this way,  
the authors achieved ‘sculpting’ of live bacterial cells into defined  
shapes<sup>3</sup> (Fig. 6D). The rod-shaped *E. coli* cells were first spher-  
5 olized in liquid medium by using the drug A22 that impedes the  
dynamics of bacterial actin MreB, which would otherwise guide  
the global cell-wall insertion pattern to maintain the rod shape.  
These cells were inoculated into PDMS microchambers, a much  
stiffer polymer than agarose, with various shapes and sizes,  
10 which were then sealed noncovalently by a layer of agarose  
containing the nutrient, A22, and cephalixin. These cells adopted  
the shapes of the microchambers by adaptive growth, where the  
ability to grow indicated the viability<sup>3</sup> (Fig. 6D). The authors used  
these cells to study the spatial adaptation of the Min proteins,  
15 which form pole-to-pole oscillations in a regular rod-shape *E. coli*  
to inhibit the cell divisions at the poles, and as a result facilitate  
the division in the cell center. The oscillations are driven by a  
Turing-type reaction-diffusion mechanism. As shown in Fig. 6B,  
MinD proteins, in their ATP-bound form, cooperatively bind to  
20 the membrane, which subsequently are bound by MinE which  
then triggers their ATPase activity and unbind MinD from the  
membrane. Intriguingly, The MinD proteins sense the cell shapes  
and align their oscillation directions to the symmetry axes  
(Fig. 6D). In addition, the time-averaged MinD concentration  
25 gradients adapt to the cell size by scaling within a characteristic  
length range of 3–6  $\mu\text{m}^3$ . These properties were proposed to be  
essential for the Min system to facilitate accurate selection of  
division axes in *E. coli* and other organisms. This method shall  
find future applications in understanding the interplay between  
30 cell shape and other subcellular structures such as protein  
clusters, cytoskeletons, and chromosomes.

## 4. Opportunities and challenges

35 The use of nanofabricated structures and microfluidics holds  
great promise for studying bacteria. Not only do they provide  
systematic and quantitative means for solving long-standing  
questions in topics such as growth, chemotaxis, and cell-fate  
switching, but they also open up new classes of studies such as  
40 investigating the roles of boundary geometry in subcellular  
organization, population dynamics and evolution. The examples  
described in this review, along with many other studies, have  
demonstrated approaches with strong modularity and transfer-  
ability. For example, individual topological modules, such as  
45 line channels, corridors, and semipermeable membranes are  
broadly applicable for studies of many other phenomena in  
bacteria. With this, studying bacteria using nanofabricated  
structures and microfluidics is growing out of its infancy.

Looking at emerging techniques, an increasing number of  
50 proof-of-principle studies indicate a broad application  
potential of simple methods that do not involve fluidic control,  
such as the ‘iChip’ (Section 2.1) and the cell-shaping methods  
(Section 3.3). These powerful single-purposed techniques will  
undoubtedly contribute to dissecting the bacterial world from  
55 the metabolic biodiversity of the natural microbial commu-  
nities to the architectural complexity of a bacterial cell.

Versatile functions can be achieved by multiplex devices that  
1 combine microfluidics with MEMS, biophysical tools, and  
synthetic genetic circuits. They enable measuring many physi-  
cal properties, such as electrical conductivity,<sup>16</sup> as well as  
5 probing the effect of force on cellular structures such as  
chromosomes.<sup>48</sup> Exciting engineering opportunities lie ahead  
in the integration of the microfluidics-based circuits that con-  
trol chemicals in space and time and the genetic circuits that  
control gene expression, quorum sensing, chemotaxis, and  
10 biofilm formation.<sup>15,37,49</sup> This will lead to building synthetic  
microbial societies that are capable of organizing into defined  
structures and execute controllable functions. From there,  
directed evolution is possible.

With the many opportunities that are not-at-all far fetched,  
15 also some challenges lie ahead. The integration of a new  
technology into a microbiology laboratory depends on whether  
it holds an absolute advantage over a conventional technique,  
and on whether the integration process is cost and labor  
friendly. For example, while microfluidics is ideal for the  
20 isolation of single-bacteria for sequencing, it currently does  
not hold a strong advantage over the encapsulation and sorting  
methods based on flow cytometry (FACS) that is commonly  
available in biology laboratories. The accessibility of nanofab-  
ricated structures and microfluidic technologies relies on their  
25 future commercialization and on collaborations between  
microbiologists and nanoengineers. Such technological inte-  
gration is greatly stimulated by cheap materials and emerging  
fabrication techniques, such as paper-based microfluidics<sup>50</sup>  
and hydrogel-based 3D printing.<sup>5</sup> In addition, customizing  
30 downstream analytic tools is essential for microbiologists to  
successfully adopt microstructure-based studies for routine  
studies. For example, geometry-related studies would benefit  
from software developed for automatic recognition of cell  
shapes or population structures in microchambers.

We look forward to the exciting new biology that will emerge  
35 from the integration of nanofabricated structures into the  
studies of bacterial life.

## Acknowledgements

40 We thank F. Hol, S. van Vliet, and Y. Caspi for their critical  
comments on the manuscript, J. Keymer, P. Galajda, and  
J. Männik for previous valuable discussions. This work was  
supported by the ERC Advanced Grant SynDiv (No. 669598), the  
45 Netherlands Organisation for Scientific Research (NWO/OCW)  
as part of the Frontiers of Nanoscience program, and Nano-  
NextNL program 3B Nanomedicine.

## References

- 1 G. M. Whitesides, *Nature*, 2006, **442**, 368–373.
- 2 K. Drescher, Y. Shen, B. L. Bassler and H. A. Stone, *Proc. Natl. Acad. Sci. U. S. A.*, 2013, **110**, 4345–4350.
- 3 F. Wu, B. van Schie, J. E. Keymer and C. Dekker, *Nat. Nanotechnol.*, 2015, **10**, 719–726.

- 1 4 J. L. Connell, A. K. Wessel, M. R. Parsek, A. D. Ellington, M. Whiteley and J. B. Shear, *mBio*, 2010, **1**. 1
- 5 J. L. Connell, E. T. Ritschdorff, M. Whiteley and J. B. Shear, *Proc. Natl. Acad. Sci. U. S. A.*, 2013, **110**, 18380–18385.
- 5 6 M. J. Madou, *Fundamentals of Microfabrication and Nanotechnology*, CRC Press, 3rd edn, 2011. 5
- 7 P. Wang, L. Robert, J. Pelletier, W. L. Dang, F. Taddei, A. Wright and S. Jun, *Curr. Biol.*, 2010, **20**, 1099–1103.
- 8 A. K. Wessel, L. Hmelo, M. R. Parsek and M. Whiteley, *Nat. Rev. Microbiol.*, 2013, **11**, 337–348.
- 10 9 R. Rusconi, M. Garren and R. Stocker, *Annu. Rev. Biophys.*, 2014, **43**, 65–91.
- 10 M. R. Bennett and J. Hasty, *Nat. Rev. Genet.*, 2009, **10**, 628–638.
- 11 Y.-J. Eun, A. S. Utada, M. F. Copeland, S. Takeuchi and D. B. Weibel, *ACS Chem. Biol.*, 2011, **6**, 260–266.
- 15 12 K. Leung, H. Zahn, T. Leaver, K. M. Konwar, N. W. Hanson, A. P. Pagé, C.-C. Lo, P. S. Chain, S. J. Hallam and C. L. Hansen, *Proc. Natl. Acad. Sci. U. S. A.*, 2012, **109**, 7665–7670.
- 13 M. A. Unger, H.-P. Chou, T. Thorsen, A. Scherer and S. R. Quake, *Science*, 2000, **288**, 113–116.
- 20 14 T. Thorsen, S. J. Maerkl and S. R. Quake, *Science*, 2002, **298**, 580–584.
- 15 F. K. Balagaddé, L. You, C. L. Hansen, F. H. Arnold and S. R. Quake, *Science*, 2005, **309**, 137–140.
- 25 16 N. S. Malvankar, M. Vargas, K. P. Nevin, A. E. Franks, C. Leang, B.-C. Kim, K. Inoue, T. Mester, S. F. Covalla, J. P. Johnson, V. M. Rotello, M. T. Tuominen and D. R. Lovley, *Nat. Nanotechnol.*, 2011, **6**, 573–579.
- 17 F. J. H. Hol and C. Dekker, *Science*, 2014, **346**.
- 30 18 S. Takeuchi, W. R. DiLuzio, D. B. Weibel and G. M. Whitesides, *Nano Lett.*, 2005, **5**, 1819–1823.
- 19 L. D. Renner and D. B. Weibel, *Proc. Natl. Acad. Sci. U. S. A.*, 2011, **108**, 6264–6269.
- 20 H. J. Kim, J. Q. Boedicker, J. W. Choi and R. F. Ismagilov, *Proc. Natl. Acad. Sci. U. S. A.*, 2008, **105**, 18188–18193.
- 35 21 D. Nichols, N. Cahoon, E. M. Trakhtenberg, L. Pham, A. Mehta, A. Belanger, T. Kanigan, K. Lewis and S. S. Epstein, *Appl. Environ. Microbiol.*, 2010, **76**, 2445–2450.
- 22 L. L. Ling, T. Schneider, A. J. Peoples, A. L. Spoering, I. Engels, B. P. Conlon, A. Mueller, T. F. Schaberle, D. E. Hughes, S. Epstein, M. Jones, L. Lazarides, V. A. Steadman, D. R. Cohen, C. R. Felix, K. A. Fetterman, W. P. Millett, A. G. Nitti, A. M. Zullo, C. Chen and K. Lewis, *Nature*, 2015, **517**, 455–459.
- 40 23 Y. Taniguchi, P. J. Choi, G.-W. Li, H. Chen, M. Babu, J. Hearn, A. Emili and X. S. Xie, *Science*, 2010, **329**, 533–538.
- 24 T. M. Norman, N. D. Lord, J. Paulsson and R. Losick, *Nature*, 2013, **503**, 481–486.
- 25 J. R. Moffitt, J. B. Lee and P. Cluzel, *Lab Chip*, 2012, **12**, 1487–1494.
- 50 26 S.-W. Teng, S. Mukherji, J. R. Moffitt, S. de Buyl and E. K. O’Shea, *Science*, 2013, **340**, 737–740.
- 27 Y. Wakamoto, N. Dhar, R. Chait, K. Schneider, F. Signorino-Gelo, S. Leibler and J. D. McKinney, *Science*, 2013, **339**, 91–95.
- 28 M. Campos, I. V. Surovtsev, S. Kato, A. Paintdakhi, B. Beltran, S. E. Ebmeier and C. Jacobs-Wagner, *Cell*, 2014, **159**, 1433–1446.
- 29 S. Taheri-Araghi, S. Bradde, J. T. Sauls, N. S. Hill, P. A. Levin, J. Paulsson, M. Vergassola and S. Jun, *Curr. Biol.*, 2015, **25**, 385–391. 5
- 30 N. Q. Balaban, J. Merrin, R. Chait, L. Kowalik and S. Leibler, *Science*, 2004, **305**, 1622–1625.
- 31 J. Männik, R. Driessen, P. Galajda, J. E. Keymer and C. Dekker, *Proc. Natl. Acad. Sci. U. S. A.*, 2009, **106**, 14861–14866.
- 32 F. Wu, E. van Rijn, B. G. C. van Schie, J. E. Keymer and C. Dekker, *Front. Microbiol.*, 2015, **6**, 607. 10
- 33 J. H. Levine, Y. Lin and M. B. Elowitz, *Science*, 2013, **342**, 1193–1200.
- 34 J. Q. Boedicker, M. E. Vincent and R. F. Ismagilov, *Angew. Chem., Int. Ed.*, 2009, **48**, 5908–5911. 15
- 35 E. C. Carnes, D. M. Lopez, N. P. Donegan, A. Cheung, H. Gresham, G. S. Timmins and C. J. Brinker, *Nat. Chem. Biol.*, 2010, **6**, 41–45.
- 36 S. T. Flickinger, M. F. Copeland, E. M. Downes, A. T. Braasch, H. H. Tuson, Y.-J. Eun and D. B. Weibel, *J. Am. Chem. Soc.*, 2011, **133**, 5966–5975. 20
- 37 A. Prindle, P. Samayoa, I. Razinkov, T. Danino, L. S. Tsimring and J. Hasty, *Nature*, 2012, **481**, 39–44.
- 38 S. van Vliet, F. Hol, T. Weenink, P. Galajda and J. Keymer, *BMC Microbiol.*, 2014, **14**, 116. 25
- 39 S. Park, P. M. Wolanin, E. A. Yuzbashyan, H. Lin, N. C. Darnton, J. B. Stock, P. Silberzan and R. Austin, *Proc. Natl. Acad. Sci. U. S. A.*, 2003, **100**, 13910–13915.
- 40 J. E. Keymer, P. Galajda, C. Muldoon, S. Park and R. H. Austin, *Proc. Natl. Acad. Sci. U. S. A.*, 2006, **103**, 17290–17295. 30
- 41 Q. Zhang, G. Lambert, D. Liao, H. Kim, K. Robin, C.-K. Tung, N. Pourmand and R. H. Austin, *Science*, 2011, **333**, 1764–1767.
- 42 F. J. H. Hol, B. Hubert, C. Dekker and J. E. Keymer, *ISMEJ*, 2015, DOI: 10.1038/ismej.2015.107, advance online publication. 35
- 43 P. Galajda, J. Keymer, P. Chaikin and R. Austin, *J. Bacteriol.*, 2007, **189**, 8704–8707.
- 44 H. Cho, H. Jönsson, K. Campbell, P. Melke, J. W. Williams, B. Jedynak, A. M. Stevens, A. Groisman and A. Levchenko, *PLoS Biol.*, 2007, **5**, e302. 40
- 45 A. I. Hochbaum and J. Aizenberg, *Nano Lett.*, 2010, **10**, 3717–3721.
- 46 J. Männik, F. Wu, F. J. H. Hol, P. Bisicchia, D. J. Sherratt, J. E. Keymer and C. Dekker, *Proc. Natl. Acad. Sci. U. S. A.*, 2012, **109**, 6957–6962.
- 47 M. T. Cabeen, G. Charbon, W. Vollmer, P. Born, N. Ausmees, D. B. Weibel and C. Jacobs-Wagner, *EMBO J.*, 2009, **28**, 1208–1219. 45
- 48 J. Pelletier, K. Halvorsen, B.-Y. Ha, R. Paparcone, S. J. Sandler, C. L. Woldringh, W. P. Wong and S. Jun, *Proc. Natl. Acad. Sci. U. S. A.*, 2012, **109**, E2649–E2656.
- 49 S. H. Hong, M. Hegde, J. Kim, X. Wang, A. Jayaraman and T. K. Wood, *Nat. Commun.*, 2012, **3**, 613. 50
- 50 A. W. Martinez, S. T. Phillips and G. M. Whitesides, *Proc. Natl. Acad. Sci. U. S. A.*, 2008, **105**, 19606–19611. 55